J Urban Health (2019) 96:235–251
https://doi.org/10.1007/s11524-018-0322-y

Urban Heat Island and Future Climate Change—Implications for Delhi's Heat

Richa Sharma · Hans Hooyberghs · Dirk Lauwaet · Koen De Ridder

Published online: 23 October 2018

Abstract UrbClim, the urban climate model, is used for short- and long-term projections of climate for Delhi. The projections are performed for RCP8.5 using an ensemble of 11 GCM model outputs. Various heat stress indices were employed to understand the role of urban heat island (UHI) in influencing the present and future urban climate of the city. UHI intensity based on 5% warmest nights (TNp95) was 4.1 °C and exhibits negligible change over time. However, the impact of UHI on other heat stress indices is very strong. Combined hot days and tropical nights (CHT) that influenced 58–70% of the reference time frame are expected to rise to 68–77% in near-future and to 91–97% in far-future time periods. For reference time period, urban areas experience 2.3 more number of heat wave days (NHWD) than rural areas per summer season. This difference increases to 7.1 in short-term and 13.8 in long-term projections. Similar to this trend, frequency of heat waves (FHW) for urban areas is also expected to increase from 0.8 each summer season in reference time frame to 2.1 and 5.1 in short- and long-term projections. The urban-rural difference for duration of heat waves (DHW) appears to increase from 1.7 days in past to 2.3 and 2.2 days in future, illustrating that DHW for cities will be higher than non-urban areas at least by 2 days. The intensity of heat wave (IHW) for urban land uses increases from 40 °C in reference time frame to 45 °C in short-term projection to 49 °C in far future. These values for non-urban land use were 33 °C during the baseline time period and are expected to increase to 42 °C and 46 °C in near- and far-future time frames. The results clearly indicate the contribution of UHI effects in intensifying the impacts of extreme heat and heat stress in the city.

Keywords UrbClim · Urban heat island · Climate change · Heat waves

R. Sharma (✉)
National Institute of Urban Affairs (NIUA), Delhi, India
e-mail: richa.sharma85@gmail.com

R. Sharma · H. Hooyberghs · D. Lauwaet · K. De Ridder
Vlaamse instelling voor technologisch onderzoek (VITO), Mol, Belgium

Introduction

Climate change is a growing concern for the nations across the world. With changing climate, the extreme events are predicted to be more frequent and severe. The number of heat waves across the globe has increased, and their duration has also been on the rise. The unusual hot summertime temperature events that occurred over an area of 0.1% of Earth's surface during the baseline years (1950–1981) now cover nearly one tenth of the global land [1]. Heat waves have severe impact on human health, and in general, heat wave-related excess mortality is more prominent among the elderly and people with pre-existing illness [2–6]. Much of these health impacts are manifested in form of cardiovascular, cerebrovascular, and respiratory diseases. Apart from mortality, heat waves also have nonfatal health impacts such as heat stroke, dehydration, and heat exhaustion that affect the labor productivity [7, 8].

According to IPCC's Fifth Assessment Report (AR-5), the heat waves are expected to be on rise till 2040 even under the RCP4.5 scenario. The models project that the frequency of warm days and nights is likely to increase with cold days and cold nights likely to decrease. The report also indicates an increase in duration, intensity, and spatial extent of heat waves for short-term projections. Also, it is very likely that heat waves will occur with a higher frequency and longer duration [9]. Heat waves have been a threat for countries across the world irrespective of temperate or tropical climates (Table 1). Since, the populations are expected to acclimatize to warmer climates in the future, by means of variety of behavioral, physiological, and technological adaptations, this might subside the extreme heat impacts to some extent. However, this may take few to several years and would require innovative adaptation measures and restructuring of health protection policies [20].

Heat waves are often described as extended periods of extreme heat. However, there is no uniform definition of heat wave with respect to the temperature threshold or the number of days used to characterize a heat wave event [21], and a number of heat wave definitions exist in literature by different authors even for same areas under study. Kent et al. [22] used 16 different heat indices with preterm birth and non-accidental death data, to study the impact of heat wave definitions on the relationship between human health and extreme heat exposure. Alexander and Arblaster [23] used two definitions of heat wave for analysing observed and future trends in extreme heat in Australia. The first definition marks a heat wave when maximum temperature is 5 °C above 1961–1990 average daily maximum temperatures for more than five consecutive days [24]. Another definition of heat wave is when maximum temperature is 5 °C above 90th percentile of daily maximum temperature (1961–1990) for more than five consecutive days [25]. This inconsistency of definitions holds true for meteorological departments of different countries. For example, in the Netherlands, heat warnings are issued when maximum temperature is expected to exceed 25 °C for at least 5 days, and of these, at least 3 days may have temperatures above 30 °C [26]. However, in the UK, average maximum temperature must be exceeded by daily maximum temperature by 5 °C for more than five consecutive days (average calculated using previous 30-year time period). While in China, the heat wave is declared when maximum temperature forecast exceeds 35 °C for two consecutive days [27]. Usually, the threshold temperature for heat wave depends on the local climate of the location under investigation and is thus higher in warmer regions. For example, in the USA, cities in colder regions experience different mortality than cities with relatively hotter weather [28]. However, this does not hold true for the European cities, where it has been found that all cities irrespective of hotter or colder summers are equally sensitive to heat waves [29].

Heat waves in general have been found to be more threatening to cities for reasons such as larger population that is exposed, physical surface properties of urban land use, additional contribution from anthropogenic heat, and pollutants [30]. Urbanisation disturbs the heat energy balance in the urban areas as compared to surrounding suburban or rural lands, resulting in differential temperature phenomenon termed as the urban heat

Table 1 List of countries, events of heat waves, and number of associated deaths

Continents/countries	Years	Loss of human lives	Reference
Europe	2003	> 70,000	Robine et al. [10]
London	2011	> 350	Green et al. [11]
Russia (Moscow)	2010	11,000	Matsueda, [12]
Australia	2009	> 370	Department of Health & Human Services [13]
US (Chicago)	1995	> 500	Whitman et al. [14]
US (California)	2006	> 600	Guirguis et al. [15]; Knowlton et al. [7]
South Korea	1994	> 3000	Kysely and Kim [16]
Japan	2010	> 1700	Nishi et al. [17]
India	2010	> 4400	Azhar et al. [18]
Pakistan	2015	> 700	Masood et al. [19]

island (UHI). The physical characteristics of urban surfaces alter the albedo and emissivity finally changing the radiative fluxes. In addition to this, with decreasing vegetation cover, the surface moisture availability decreases as well. The complicated geometry of the urban streets and tall buildings modifies the near-surface flows further adding to the urban heat. Thus, at night, while rural areas cool down, the urban areas are slow in releasing the heat absorbed during the day [31]. These nocturnally sustained temperatures that result in lack of relief at night pose greater threats to human life as the body does not get time to recover from the exposure of extreme heat. This additive effect of UHI exacerbates the impacts of such events in urban areas as compared to surrounding suburban and rural areas [32, 33]. This enhances the probability of occurrence of extreme heat events in urban areas and also exaggerates the heat wave impacts. UHI is more prominent in areas which lack green cover and have higher anthropogenic emissions or are densely populated with high buildings. UHI has been credited with contribution to the 2015 heat wave event in Karachi [19, 34, 35].

Urban areas are expected to grow and the cities across the world will undergo expansion and regeneration. The way in which cities influence their own climate is complex. However, at the same time, it is important to appreciate this relationship and apply this knowledge in urban planning to make cities more adapted and resilient to the climate change.

Indian cities too have been experiencing heat waves. The rapid population growth along with changing climate is expected to further intensify the problem. Over the past decade (1990–2009), the mean annual temperatures across India have increased up to 1 °C in comparison with historical average, computed from 1961 to 1990 [36]. In May 2010, the city of Ahmedabad was hit by a deadly heat wave killing more than a 1000 people [18]. This eventually resulted in the development of the first Heat Action Plan by the Ahmedabad Municipal Corporation (AMC) that consisted of two phases [37]. The first phase explored the causes for heat wave mortality, and the second phase focussed on raising awareness and also creating the alert levels to inform people well in advance. It has been found that most heat-related death could be prevented with adaptation measures such as efficient warning systems and emergency planning.

As per the IPCC AR5, with the climate changing, heat-related mortality in developing countries may be considered more significant, as population in cities of these nations (such as Mexico City, New Delhi) lacks the resources required to adapt, making them more vulnerable to impacts of heat waves. The report also points that majority of the research publications regarding heat waves refer to cities in developed countries [9]. If cities need to prepare adaptation strategies for a changing climate, heat waves in this case, decision makers, and city planners and managers need quantitative projections. However, most of the future climate studies and projections focus more on regional or country levels. Very limited studies are available that analyze future projections at the scales of a city. Most of the studies focus on analysing merely warm days or nights [9]. Most of such studies have been conducted in developed countries with temperate (e.g. European cities (Guerreiro et al., [38])) or tropical to subtropical climates, e.g. Tokyo (Adachi et al., [39]) and Sydney [40]. There exists a huge gap in literature on such studies with respect to cities located in developing nations with arid or semi-arid climate conditions such as Delhi. Cities that are already experiencing very hot and dry summers and due to low adaptive capacities are more vulnerable to changing climate.

This study aims at analysing the impacts of climate change on the city's climate with respect to background heat contributions from the UHI effect. Addressing the issues discussed above, the future climate scenario for the city of Delhi was simulated, analysing the extreme heat conditions in near- and far-future time frames and comparing them with the reference time period.

Study Area—Delhi

Delhi is the capital city of India, with a population of nearly 21 million as per the census of 2011. Though India is more of a tropical country, Delhi, however, is a land locked city in the Indo-Gangetic plains of north (Fig. 1). The city has cold winters with chilling winds blowing in the north from Himalayas. Conversely, the summers in the city are very hot with dry hot winds blowing from Thar Desert in the south, which exposes the city to extreme heat waves. The summer months last from second half of April till July beginning, when monsoon showers bring relief to the parched soils. With a very high density of population and its semi-dry climate, the city's population is highly vulnerable to extreme heat impacts.

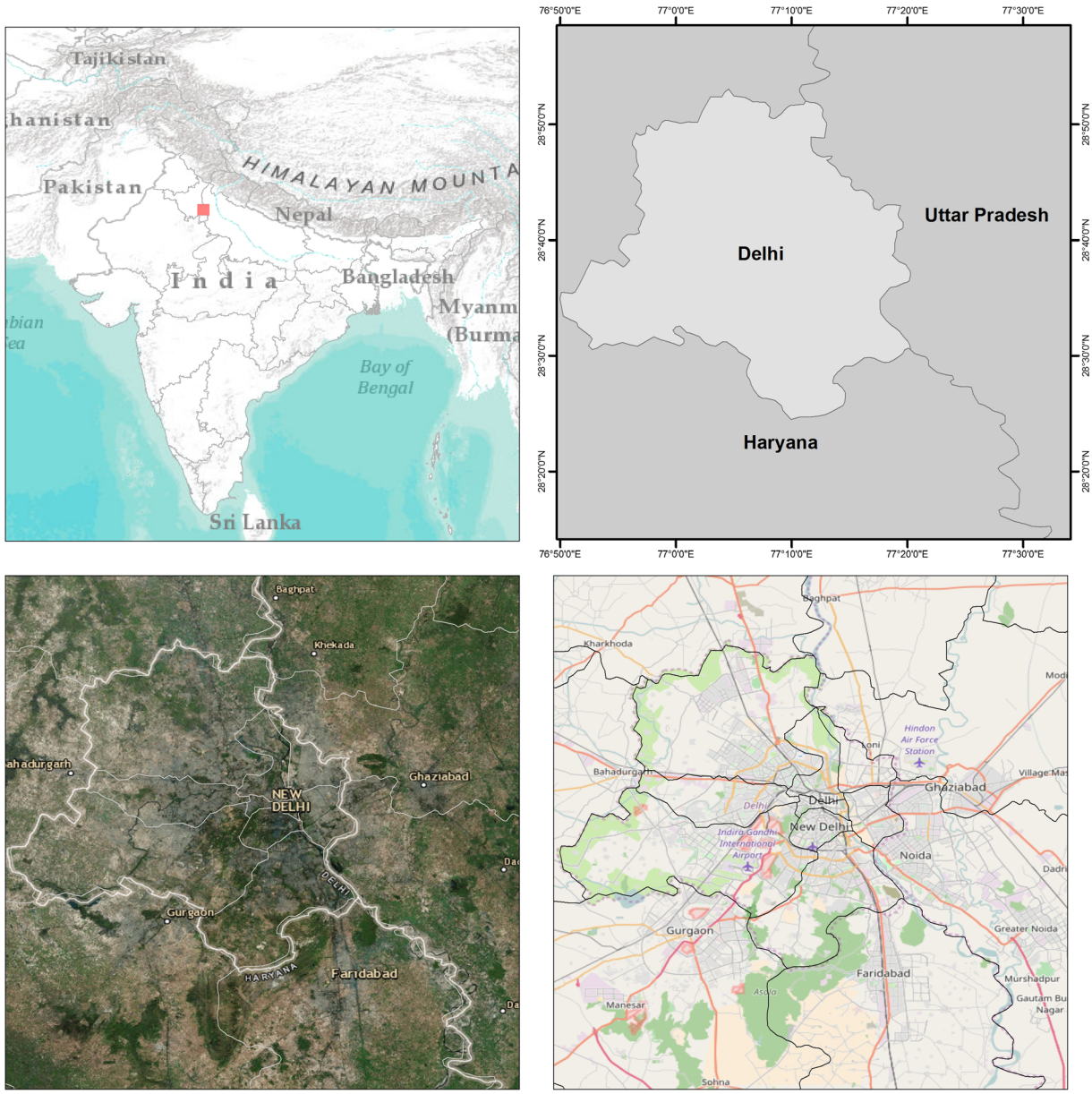

Fig. 1 The study area location, and the satellite and OpenStreetMap views

Methodology and Data

Model Setup and Evaluation

UrbClim is the urban climate model based on a land surface scheme containing a bulk parameterisation of the urban surface energy balance also accounting for anthropogenic heating [41], coupled to an atmospheric boundary layer scheme. The model is capable of simulating longer time periods at a high spatial resolution (order of 100 m), at an affordable computational cost, while not compromising on accuracy. The model has been applied to and successfully validated for a number of cities [42–45].

In order to simulate the climate of the wider urban agglomeration of Delhi and to evaluate the performance of UrbClim, the model is run for a 1-year reference period (2014). The model is driven directly with meteorological data from the ERA-Interim reanalysis of the European Center for Medium-range Weather Forecasting

(ECMWF), for a domain configured with 81 × 81 grid cells in the horizontal direction, using a spatial resolution of 1 km [42, 44]. In the vertical direction, 20 levels are specified, with the first level 10 m above the displacement height, the resolution smoothly decreases upward to 250 m at the model top located at 3 km height. This vertical discretisation closely matches that of the ECMWF host model. Terrain elevation data are taken from the GMTED2010 Dataset [46], which has a global coverage. The spatial distribution of land cover types, needed for the specification of required land surface parameters, is taken from the Local Climate Zone (LCZ) map generated using WUDAPT's methodology [47]. The World Urban Database and Access Portal Tools (WUDAPT) is an international collaborative project that initiates collection of data focusing on form and function of cities across the globe [48]. The LCZ scheme employed by WUDAPT comprises of 17 zones based on surface structure (e.g. building and tree height and density) and surface cover (pervious versus impervious). Of these 17, the first three categories (1–3) characterize the tightly packed buildings with little green space, and the next three classes cover less densely packed buildings with relatively more green cover. Classes 7, 8, and 9 cover lightweight low-rise, large low-rise, and sparsely built land use classes. The remaining seven classes (A to F) refer to natural cover types with the exception of paved surfaces.

The LCZ classification types are translated to the UrbClim land cover classes specifying values for the soil sealing fraction and the roughness length for momentum for each LCZ class. Other required parameter values (e.g. albedo, emissivity) are specified conforming to the standard UrbClim values [42]. Maps of vegetation cover fraction are obtained from the normalized difference vegetation index (NDVI) acquired by the MODIS instrument on-board the TERRA satellite platform. Vegetation cover fraction is specified as a function of the NDVI using a linear relationship proposed by Gutman and Ignatov [49] and then interpolated to the model grid. Non-urban land use model grid cells are divided into vegetation and bare soil. In contrast to previous applications of the model in European cities (e.g. Lauwaet et al. [44]), for Delhi, the vegetation cover fraction is given priority over the soil sealing fraction if they happen to sum up to over 100% in a model grid cell. A detailed description of the original model could be found in De Ridder et al. [42].

Weather station data from Safdarjang Airport and Indira Gandhi International (IGI) Airport was procured from NOAA's National Climate Data Center (NCDC) for evaluation of the model. T2M values were extracted from the model outputs for corresponding locations and times and compared with observation values. The basic statistics for the modelled and observed T2M values are compared for the two airport locations. The average daily minimum values for UrbClim are 19.69 °C for Safdarjung and 20.28 °C for IGI, and for observed values, it is 19.98 °C for Safdarjung and 19.32 °C for IGI. On the other hand, the average daily maximum of the modelled values (30.79 °C for Safdarjung and 30.77 °C for IGI) is slightly greater than the observed maximums (29.62 °C for Safdarjung and 29.9 °C for IGI). RMSE values for Safdarjung in general are smaller than that for IGI airport. The root mean square error of 2.2–2.6 °C for the T2M air temperature simulated for Delhi.

In addition to using the 2-m air temperature (T2M) outputs for the airports, land surface temperature (LST) outputs were also used for validation purposes, as satellite data offers a synoptic coverage. UHI validation is performed for comparing MODIS LST products against UrbClim LST outputs. Analysis of the mean magnitude for all UrbClim and all MODIS images indicates that UrbClim marginally overestimates the surface urban heat island (SUHI) intensity. Mean UrbClim SUHI (1.99 °C) is slightly overestimated for Aqua (1.88 °C) and is (1.77 °C) underestimated for Terra (1.93 °C) MODIS LST images. During day, the mean UrbClim SUHI at Terra and Aqua hours is 0.47 °C and 1.21 °C in contrast to 0.87 °C and 0.84 °C for MODIS Terra and Aqua LST. At night, UrbClim SUHI is overall lower (2.43 °C and 2.39 °C) compared to the corresponding Terra (2.53 °C) and Aqua (2.42 °C) images. In spite of great heterogeneities in land use of the city (a typical feature of cities in developing countries), the model's performance is quite satisfactory with Index of Agreement (IoA) ranging from 0.79 to 0.98.

Future Simulations

The Fifth Assessment Report (AR-5) of the Intergovernmental Panel on Climate Change (IPCC) has identified a new set of four climate scenarios called Representative Concentration Pathways (RCPs): RCP8.5, RCP6, RCP4.5, and RCP2.6. These scenarios take into account future emissions, concentrations, land use, and radiative forcing levels in three different time frames: 'Reference' from past (1985–2005), the 'Near Future' (2026–2045), and the 'Far Future' as end-of-century time frame (2081–2100).The prominence of these

scenarios largely depends on the mitigation policies, and each scenario has an underlying set of assumptions. Of the four RCPs, RCP8.5 usually gets the most attention.

RCP8.5 is based on the MESSAGE model and IIASA Integrated Assessment Framework by the International Institute for Applied Systems Analysis (IIASA), Austria. One of the first assumptions in RCP8.5 is regarding the population growth; the population will grow in accordance with the high end of the current UN forecasts [50]. Other assumptions are with respect to technology and energy consumption with increasing coal dependency and slight improvements in energy efficiency. In conclusion, RCP8.5 is important in as it warns against complacency and offers an idea about the extreme outcomes [51]. Thus, for the current study, RCP8.5 scenario was chosen, and three time periods chosen for simulation were consistent with IPCC time frames.

For the reference time frame or past, ERA-interim forcing was used for simulations for the years from 1986 to 2005 and the outputs were considered as baseline. For future simulations, the statistical rescaling methodology was followed [45]. For distant future simulations, GCM outputs were used in place of ERA-Interim forcing. It is not advisable to use only one GCM model [9] as the agreement between ensemble means and climate data is much higher than that with any single climate model. Thus, an ensemble of 11 GCM model outputs from different institutes was chosen that contain all the required parameters at suitable time increments, such that these appropriately account for the uncertainty associated with the global climate projections.

The statistical rescaling method was employed to simulate future climate for the city. The details of this method could be found in Lauwaet et al. [45]. The validity of the statistical method has been established by Lauwaet et al. [45], by comparing the simulated urban climate projections (for future) with the statistically rescaled results (for same time frame). The method has been found to have advantages of lesser computation time and smaller data amounts required which makes this method very efficient and quick. For the current study, the summer months of April, May, June, and July were chosen to study the role of UHI in aggravating the extreme heat impacts on the city in future climate scenarios.

Heat Stress Indices

Temperature data for the baseline and future periods is assessed using five broad types of indices to determine the changes in the intensity of daily summer temperature extremes. The indices were chosen in a manner that they represent the variety of temperature characteristics, their extreme behaviours and their importance in terms of impact for human health. Table 2 gives a list of temperature indices used, their type, codes, and brief descriptions [25]. Most of these indices have been used in previous studies [52–57] and are recommended by the World Meteorological Organization, the project on Climate Variability and Predictability (CLIVAR), and the Expert Team on Climate Change Detection, Monitoring and Indices (ETCCDMI). For convenience of the reader, in the following section, minimum temperature is symbolized as T_{min}, maximum temperature as T_{max}, and average temperature as T_{avg}.

The first type of indices makes use of *absolute temperature* values. These include 'Coldest Night' (TNn), 'Coldest Day' (TXn), 'Hottest Night' (TNx), and 'Hottest Day' (TXx). These represent the coldest night, coldest day, hottest night, and hottest day temperature values for each grid cell over the respective time frame [52]. The second type of indices is more statistical in nature and is *based on percentile* values. Occurrence of 'warm nights' falls under this category of indices. This estimates heat stress using 5% warmest nights determined as 95th percentile of the T_{min} for all the days in the respective time frame. This index is further used to compute UHI intensity for the given time periods under consideration [45]. 'Combined hot days and tropical nights' (CHT) is a *threshold based index*. Such indices are defined as the number of days when temperature values are above and/or below a fixed threshold. This index shows the average count of combined occurrence of hot days (T_{max} exceeding 35 °C) and tropical nights (T_{min} exceeding 20 °C) for each grid cell [54].

Duration indices define periods of excessive heat. Under this category, we used four basic indices, all of which are based on the heat wave identification. These include, 'number of heat wave days', 'number of heat waves (or frequency)', 'average duration of heat wave events', and 'average intensity of heat wave events' [54]. An event of heat wave in this study is marked when both the 3-day running average for T_{min} and 3-day running average for T_{max} exceed their respective thresholds. These thresholds are 98th percentile (temporal) of rural minimal (10th percentile of T_{min} in spatial domain) during summer periods in reference time period and 98th percentile (temporal) of rural maximal (10th percentile of T_{max} in spatial domain) during summer

Table 2 List of heat stress indices, their types, codes, and description

Type	Name	Code	Description
Absolute values	Coldest night	TNn	Minimum of daily minimum temperature
	Coldest day	TXn	Minimum of daily maximum temperature
	Hottest night	TNx	Maximum of daily minimum temperature
	Hottest day	TXx	Maximum of daily maximum temperature
Percentiles	UHI intensity based on 5% warmest nights	TN95	The pixels experience a warm night, when TN for that pixel is greater than 95th percentile of TN (TNp95)
Threshold	Combined hot days and warm nights	CHW	Number of days when days are hotter than 35 °C and nights are hotter than 20 °C
Duration	Number of heat wave days	NHWD	Average number of days of heat wave each year
	Frequency of heat wave events	FHW	Frequency of occurrence of heat wave each year
	Average duration of heat wave events	DHW	Average number of days a heat wave persists
	Average intensity of heat wave events	IHW	Maximum of average temperature of heat wave days

periods in reference time period respectively. For the current study, these thresholds are found to be 30 °C and 45 °C respectively. Using this definition, days of heat wave event are identified and are then used to compute the four indices. For estimating average intensity of heat waves, temporal maximum of T_{avg} of heat wave days was determined. Most definitions for intensity estimation use maximum temperatures. However, since heat wave event is a function of both minimum and maximum temperature, it is more suitable to use both maximum and minimum temperatures to estimate intensity and not just depend on maximum temperatures. Also, it is to be noted that the city of Delhi is surrounded by agricultural fields that lay fallow in summer months, which thus tremendously increases the day time temperatures over these bare lands (sometimes higher than the city temperatures). However at night, these lands cool down drastically. Thus the areas where average temperatures are high (i.e. both day and night temperatures) seem to be more vulnerable to heat wave impact as the night time recovery for population in these areas is stifled. Hence, we used average temperature to estimate intensity of the heat wave events.

Results and Discussion

Future UHI

In this study, the UHI effect over the city domain is assessed using indicators based on heat stress indices explained above. These include the UHI Intensity

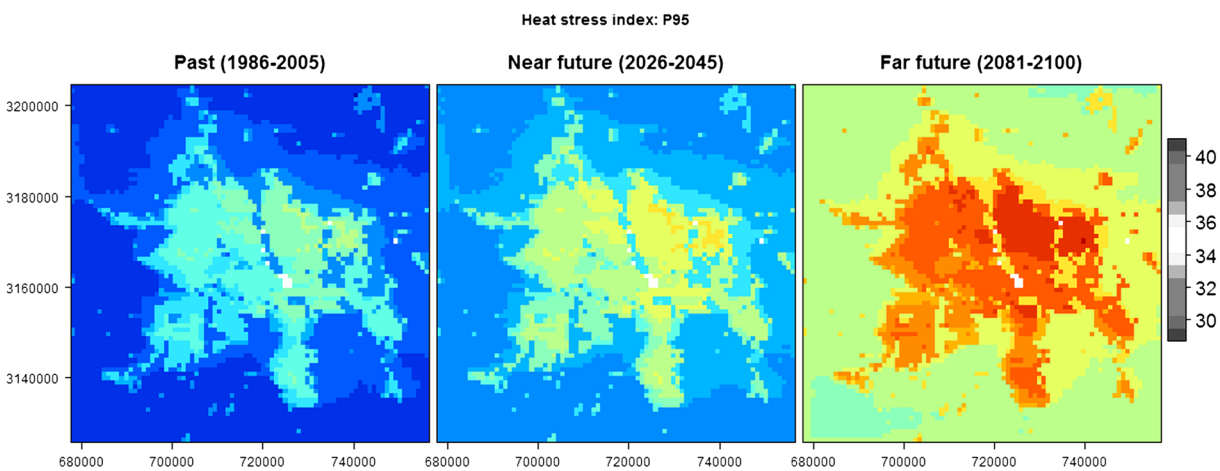

Fig. 2 Heat index TNp95 (95th percentile of T_{min}) for the three time frames.

indicator which is based on urban and rural temperature difference for warm nights, where warm nights are assessed using 95th percentile (TNp95) of the daily minimum temperature (T_{min}). For analysing UHI intensity (or UHII), it is important to consider night time temperatures (T_{min}), for a city like Delhi, where dry conditions prevail.

In addition to TNp95, other heat stress indices are also analyzed for understanding the impacts of UHI on urban climate in contrast to rural grid cells in the domain. Urban and rural pixels are determined from 'warm nights' (computed above) as 90th and 10th percentiles respectively, and their difference gives the UHI intensity (UHII). Based on this, the UHI for base years (1986–2005) is 4.11 °C and is observed to be 4.08 °C and 4.12 °C for the time frames of near (2026–2045) and far future (2081–2100) (Fig. 2). Though there is not a substantial change in the intensity of UHI, however, this difference in urban and rural temperatures makes urban areas of the domain more vulnerable to extreme heat. Similar results have been reported by McCarthy et al. [58], Oleson [59], and Lauwaet et al. [44] where they observed that even though there will be increased warming under future climate scenarios but the UHI will remain more or less the same.

Since, urban area is warmer than rural land by nearly 4 °C; they are exposed to more severe heat hazard than their rural vicinities. In other words, when rural areas experience 35 °C during warm nights in far-future scenario, the city will be exposed to 39.1 °C, which can cause much more health hazards.

To understand the effect of different urban LCZ on UHI and HW in the future, different indicators were calculated for various LCZ. For this analysis, LCZ 1–3 were combined to extract compact urban, LCZ 4–6 were merged to obtain open urban, and the third urban category to be analyzed was sparse-built (LCZ 9). Broadly, these three categories have been analyzed as they account for the densities of built-up which largely governs the urban planning in Indian cities. UHII extracted for these three urban forms are presented in the Fig. 3.

For analysing the LCZ-based UHI, mean rural temperature values were subtracted from the masks of each urban form (compact, open, and SB) for each time frame. It was observed that the UHII values for each form did not change much over the years as observed for overall UHI. UHII for compact is observed to be 3.1 ± 0.1 °C for the urban compact over the years, while for open urban built, it ranges between 2.48 °C and 2.5 °C, and the range is 1.32–1.33 °C for sparse-built. The results clearly indicate that with increasing density of urban built, the UHI intensity increases. Open LCZ appears to be 1.2 °C warmer than sparse-built and compact urban built is further warmer by 0.61 °C.

Spatio-Temporal Changes in Heat Stress Indices

This sub-section deals with analysing the different heat stress indices in reference, near-, and far-future time frames. The indices have been used to understand the role of UHI in aggravating the climate vulnerability of urban areas to and heat stress. Apart from UHI intensity (discussed in previous sub-section), other indicators for the heat stress indices have been calculated to understand the cumulative effects of climate change and UHI on the city's climate. These indicators include determining urban and rural values for these indices and their differences as well.

Of the various indices, the 'Coldest Night', 'Coldest Day', 'Hottest Night', and 'Hottest Day' indices have more or less the same UHI indicator values over the years. The 'Coldest Nights' are expected to get warmer by 2 °C in 2026–2045 and further by 3.7 °C by 2081–2100. Similar trend is expected for 'Coldest Day', 'Hottest Day', and 'Hottest Night'. The increase in temperature for these indices is expected to be 1.5 °C, 1.1 °C, and 1.1 °C from reference to near future respectively. And from near future to far future, temperature for 'Coldest Day', 'Hottest Day', and 'Hottest Nights' is projected to further increase by 3.5 °C, 3.9 °C, and 4.2 °C respectively (Fig. 4). Thus over the years, the maximum and minimum temperatures are increasing at similar pace for both urban and rural areas, and hence the difference between them stays relatively constant. But due to this difference in temperature, urban areas reach the threshold more often than rural areas and hence experience extreme heat events more often. Another interesting fact is the different UHI indicator values these indices exhibit. Night time indices (coldest and hottest night) more prominently illustrate the UHI effect evident from values given in Table 3. UHI value is the highest for coldest night (5.9–6 °C) and the hottest night (5.7 °C) followed by the coldest day (0.9 °C). It is interesting to observe that the hottest day UHI is actually slightly negative indicating that rural areas experience maximum temperature that is 0.6–0.7 °C higher than that from urban areas. Similar results have been observed by Lemonsu et al. [60] in Paris reporting a

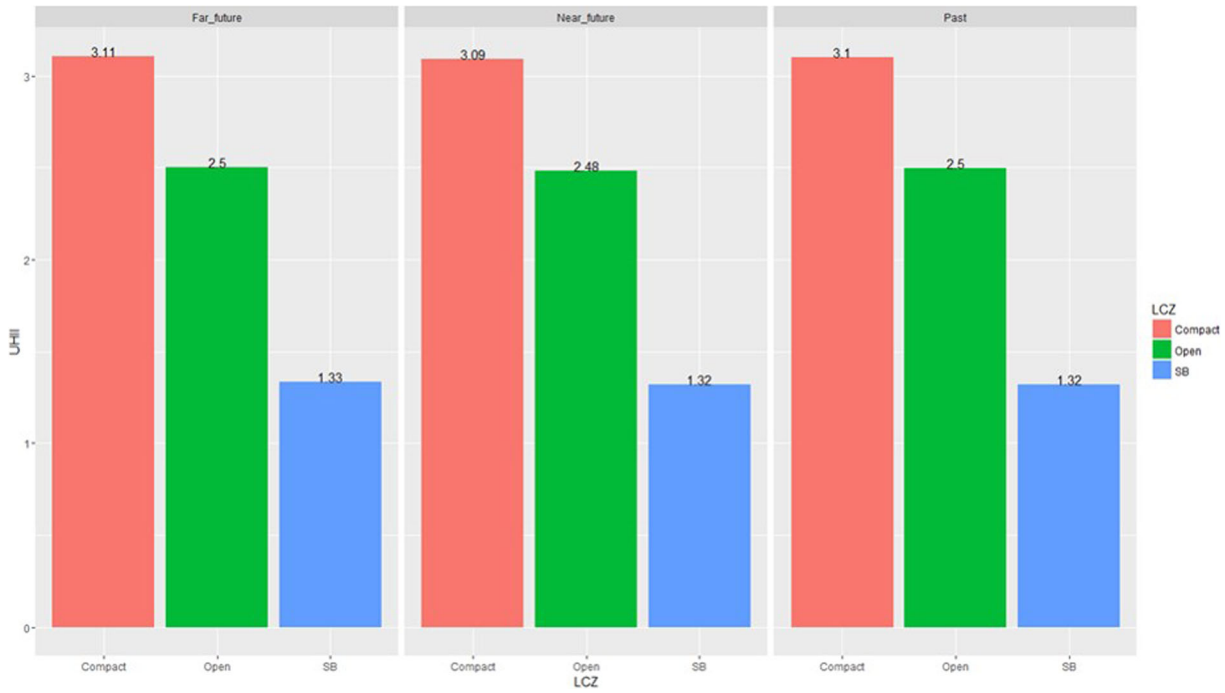

Fig. 3 UHII for compact, open and sparse-built urban forms for the three time periods.

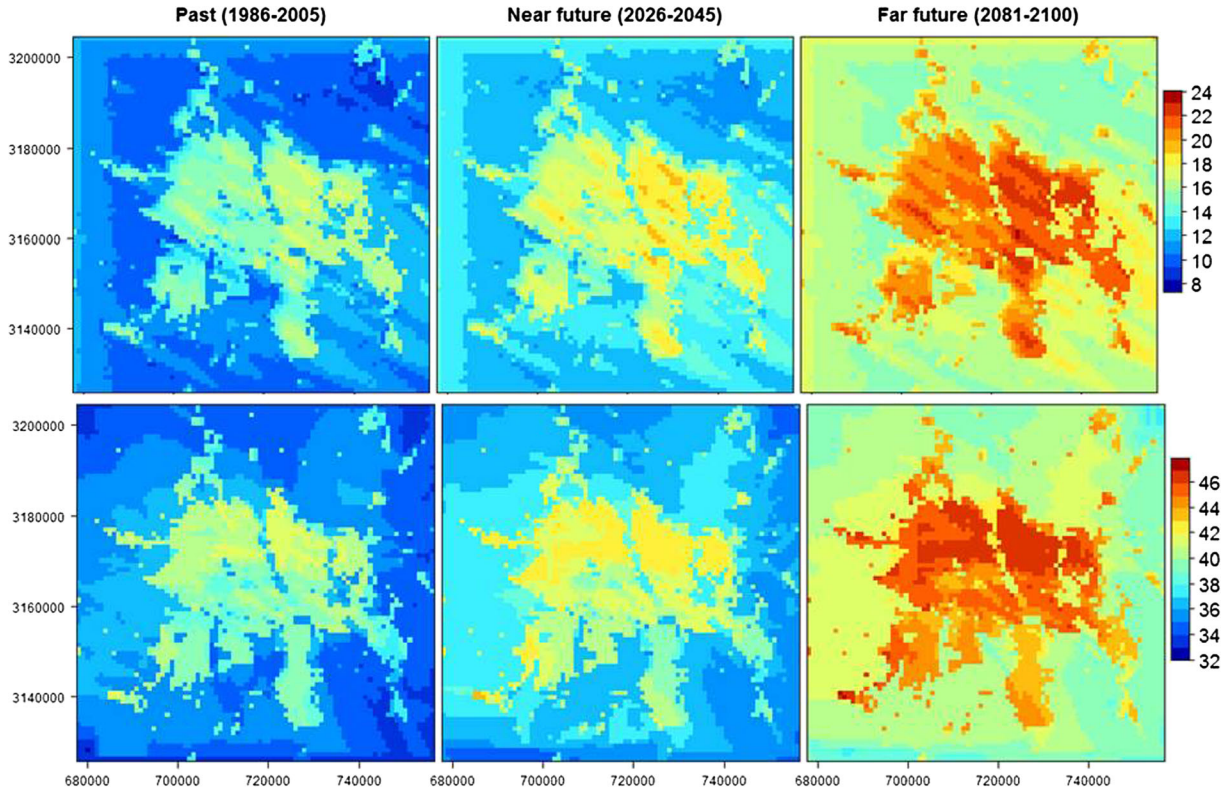

Fig. 4 'Coldest Night' temperature (upper panels) and 'Hottest Night' (lower panels) temperature for time frames of reference/past (1986–2005), near future (2026–2045), and far future (2081–2100).

Table 3 Heat wave indices used in the study, the urban (P90) and rural (P10) values, and respective UHI indicator (Δ)

		Urban	Rural		UHI indicator
TNn				ΔTNn	
	1986–2005	15.5	9.8		5.7
	2021–2045	17.4	11.7		5.7
	2081–2100	21.1	15.4		5.7
TXn				ΔTXn	
	1986–2005	22.5	21.8		0.9
	2021–2045	24.1	23.3		0.9
	2081–2100	27.6	26.8		0.9
TNx				ΔTNx	
	1986–2005	40.1	34.2		5.9
	2021–2045	41.2	35.7		5.9
	2081–2100	45.4	39,4		6
TXx				ΔTXx	
	1986–2005	47.9	48.5		−0.7
	2021–2045	49	49.6		−0.6
	2081–2100	52.9	53.5		−0.7
CHT				ΔCHT	
	1986–2005	84.5 (69.3%)	72.9 (59.8%)		11.6 (9.5%)
	2021–2045	92.5 (75.8%)	84(68.9%)		8.5 (7%)
	2081–2100	117.3 (96.2%)	113 (92.6%)		4.8 (3.9%)
NHWD				ΔNHWD	
	1986–2005	3.5	0.6		2.9
	2021–2045	10.6	3.5		7.1
	2081–2100	47.5	33.7		13.8
FHW				ΔFHW	
	1986–2005	1	0.3		0.7
	2021–2045	2.1	1.1		1
	2081–2100	5.05	4.25		0.8
DHW				ΔDHW	
	1986–2005	3.5	1.6		1.9
	2021–2045	5.3	3.1		2.2
	2081–2100	9.7	7.5		2.2
IHW				ΔIHW	
	1986–2005	39.8	33.1		6.7
	2021–2045	44.9	42.1		2.8
	2081–2100	48.7	46		2.7

decrease in UHI by the end of the century. While Hamdi et al. [61], observed that in Brussels in spite of increased warming in the city under future climate scenario, effect on UHI was neutral.

UHI indicators based on absolute value indices (Table 2) do not show variation over the years. However, other heat stress indices highlight the impacts of UHI on city's climate. 'Combined hot days and tropical nights' (CHT) gives the percentage of days in a summer season when the days temperature is above 35 °C and night time temperature is above 20 °C, where day temperature is represented by T_{max} and night temperature by T_{min}. CHT has often been associated with excess mortality during extreme heat episodes [54] due to

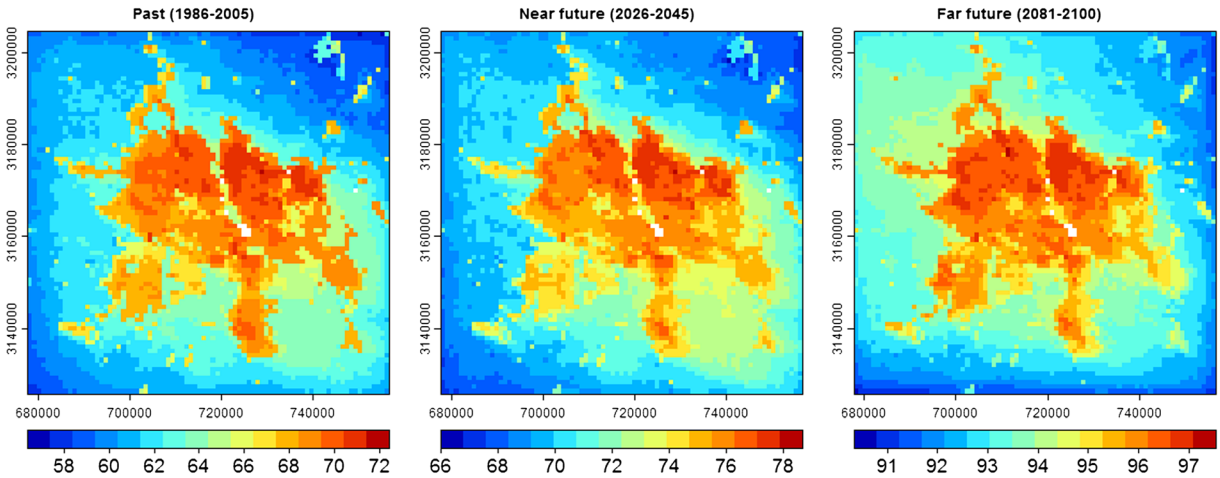

Fig. 5 Combined hot days and tropical nights for the three time frames

consecutive occurrence of days and nights when temperature is > 20 °C. During the baseline years, 58–70% of the days of the summer season fell under CHT, which is expected to increase to 68–77% in near future, and this percentage is further expected to rise to 91–97% in far-future time periods (Fig. 5). The UHI indicator for CHT (ΔCHT) suggests that over the time, the gap between CHT percentage for urban and rural falls. However, the overall CHT is increasing for both urban and rural and even in far-future urban areas will experience 4% more CHT than rural neighborhood. Another fact that emerges from this analysis is that by end of the century the city areas will experience CHT for almost 97% of the summer days. The northern and eastern parts of the city seem to be consistently experiencing highest number of CHT throughout all the three time frames.

The next set of indicators is based on *heat wave* (*HW*) indices (number, frequency, duration, and intensity). For this study, a heat wave event is defined as days when 3-day average for T_{min} and T_{max} is greater than their respective 98th percentiles. Based on the identified heat wave days, average number of such days over each time frame is estimated, to get number of heat wave days (NHWD) each summer month (Fig. 6). UHI indicator for NHWD (ΔNHWD) gives a difference between NHWD for urban and rural areas. This indicator was 2.3 (per summer season) for past time period, that is the urban areas witnessed heat wave for 2.3 more days as compared to rural areas. This is expected to increase to 7.1 in short-term projection. The city in the study domain is further expected to experience 13.8 more days of heat wave in comparison to rural areas in far-future time

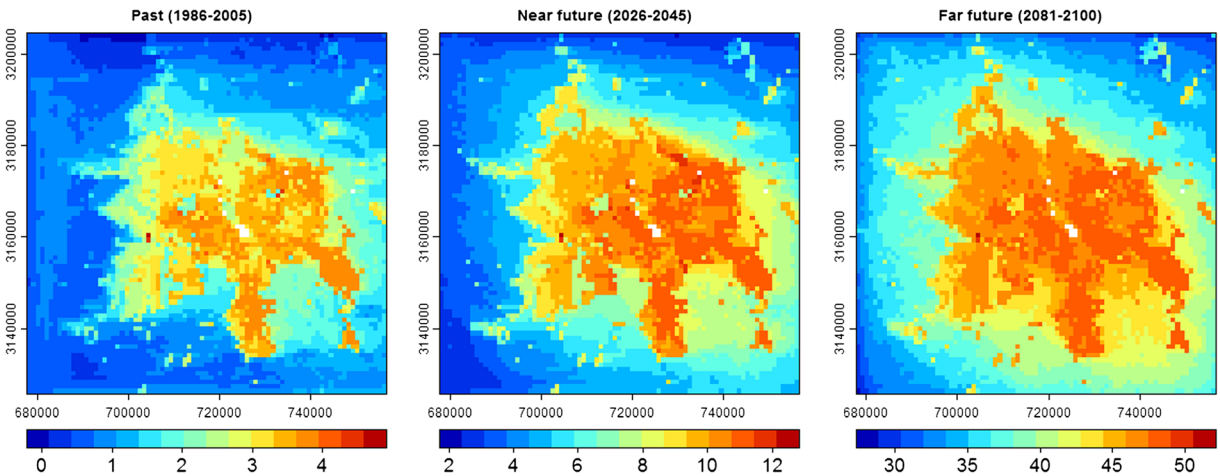

Fig. 6 Number of heat waves days during reference, near, and far future

frame. This is a clear indication of impact of UHI on the city's local climate. Another important index of heat stress with respect to heat waves is the frequency of occurrence of heat wave events (FHW). Similar to the trends of NHWD, FHW for urban areas is also expected to increase from 0.8 in reference time frame to 2.1 and 5.1 in short- and long-term projections respectively. ΔFHW suggests that if rural areas experience 22 HW events in near future then, the city will be facing 42 such events. And in far-future time frame, this difference is expected to be 16 HW events. Though, ΔFHW slightly decreases from near to far future, but the NHWD increases. This signifies that the HW event in far future will comprise of higher number of days and for each event the population will be exposed to extreme heat for longer duration. Similar results have been observed for several cities of the UK, by McCarthy et al. [58]. The researchers report that the intensity of UHI remained constant; however, the instances of extreme heat events and heatwaves are almost twice as higher in the cities.

Along with number of days and frequency of heat waves, another important index indicating heat stress is the average duration of heat waves (DHW), i.e. on average for how long each heat wave event prevails. This is significant from health perspectives as this prolongs the exposure time without sparing enough time for body to recover increasing chances of health impacts such as heat strokes. For urban grid cells in the domain, the DHW in near future is expected to be 5.3 days in near future and 9.7 towards the end of the century time frame comparison to 3.3 days during reference period. The UHI indicator for DHW (ΔDHW), appears to increase from 1.7 days in past to 2.3 and 2.2 days in future, illustrating that DHW for cities will be higher than non-urban areas at least by 2 days.

Intensity of heat wave (IHW) is also considered very important from perspectives of extreme heat stress exposure to human population. The IHW for urban land uses increases from 40 °C in reference time frame to 45 °C in short-term projection time period to 49 °C in far future. These values for non-urban land use were 33 °C during the baseline time period and are expected to increase to 42 °C and 46 °C in near and far-future time frames. Thus UHI indicator for IHW (ΔIHW) is 7 °C for past and is expected to decrease to 3 °C in future. However, this is not an indication of diminishing UHI effect as intensity of heat wave should not be considered in isolation [62]. Studies also suggest that extended periods of extreme temperatures increase risk beyond that associated with single days of high temperatures [3, 63]. Son et al. [62], also show that heat wave mortality risk increased by 3.5% for every 1 °C increase in average daily mean temperature during heat waves. While, this estimated increase in mortality is 26.2% for a 1-day increase in the duration of heat wave. Díaz et al. [64] showed that mortality increases exponentially with heat wave duration. Thus, while, UHI indicator for IHW decreases, a steady and drastic increase in frequency, duration, and length UHI indicators signify, more deadly heat wave exposures in urban areas.

Urban form (compact, open, and sparse-built)-based analysis of various HW indicators was performed to understand the response of these urban forms to the warming climates. The intensity and length of the heatwaves (IHW and LHW) do not seem to vary too much with the varying urban forms. For rural areas, the average intensity of heat wave (IHW) is observed to be 35.5 °C, which for compact, open, and sparse-built (SB) is 39 °C, 39.4 °C, and 39.1 °C. Similar patterns are detected for near and far future with 43 °C as the rural IHW, and 44.5–44.7 °C as the IHW for the three urban forms. The IHW is expected to further rise to 46.9 °C in far future for rural parts, while for urban parts (compact, open, and sparse-built), the same is expected to range from 48.3 to 48.6 °C. The average length of heat wave is observed to be 2 days for rural and 3 days for urban (all the three forms). The same is expected to be 4 and 5 days respectively in near future. The length is further expected to increase in far future to 8 days for rural and 9 and 10 days for compact, sparse-built, and open urban forms respectively.

It is interesting to note that the frequency of heat waves (FHW) increases moving from rural to compact then to open and to sparse-built in all the three time frames. Similar trend is observed for the number of heat wave days (NHWD) experienced each season. Length of heat waves (LHW) is consistently a day higher in urban areas as compared to rural areas; however, it does not vary between different urban forms. Analysing coldest day, it is observed that the temperature decreases from compact to open to sparse-built. For instance, the coldest day is observed to be 22.2 °C for rural, 22.7 °C for compact urban, 22.5 °C for open urban, and 22.2 °C for sparse-built urban areas. The values are expected to rise to 23.7–27.2 °C for rural areas in near and far future. During the same time frames, the values for compact, open, and sparse-built are expected to be 24.2–27.7 °C, 24–27.5 °C, and 23.7–27.3 °C. Similarly, for the coldest

night, temperature values range from 11.1–16.7 °C in rural areas (from past to near and far future). For sparse-built urban areas, the same ranges from 13.2–18.8 °C, for open urban areas these values lie between 14.9–20.5 °C and for compact urban the values range between 15.7 °C and 21.3 °C. For hottest night, the temperature values show similar trend with warming increasing as moving from rural (35.5–40.8 °C) to sparse-built (38.5–43.8 °C), to open (39.4–44.7 °C), and to compact (40–45.4 °C) urban areas. Temperature for the hottest day does not vary too much from rural to the three urban forms. These results indicate how increasing proportion of built-up increases vulnerability of the area to heat stress and extreme heat events (Table 4).

Table 4 Average values for various heat stress indices for different urban forms (compact, open, and sparse-built) and the rural land use

		Rural	Compact	Open	SB
IHW (°C)	Past	*35.5*	39.0	39.4	39.1
	Near	*43.0*	44.7	44.7	44.5
	Far	*46.9*	48.6	48.6	48.3
FHW (per season)	Past	*11*	17	19	20.8
	Near	*31*	35.1	38.0	41.5
	Far	*93*	99.0	98.5	100.1
LHW (days)	Past	*2*	3	3	3
	Near	*4*	5	5	5
	Far	*8*	9	10	9
NHWD (days)	Past	*26.6*	53.5	61.6	64.0
	Near	*117.5*	187.5	197.7	201.6
	Far	*773.6*	925.6	930.3	934.0
Coldest day (°C)	Past	*22.2*	22.7	22.5	22.2
	Near	*23.7*	24.2	24.0	23.7
	Far	*27.2*	27.7	27.5	27.3
Coldest Night (°C)	Past	*11.1*	15.7	14.9	13.2
	Near	*13.0*	17.6	16.8	15.1
	Far	*16.7*	21.3	20.5	18.8
Hottest Day (°C)	Past	*48.1*	47.7	47.8	48.0
	Near	*49.1*	48.7	48.8	49.0
	Far	*53.1*	52.7	52.8	52.9
Hottest Night (°C)	Past	*35.5*	40.0	39.4	38.5
	Near	*37.1*	41.5	40.9	40.2
	Far	*40.8*	45.4	44.7	43.8
Tmin95 (°C)	Past	*30.6*	34.1	33.5	32.7
	Near	*32.2*	35.7	35.1	34.3
	Far	*35.8*	39.4	38.8	38.0
NCHT (unitless)	Past	*62.5*	69.7	68.6	67.1
	Near	*70.9*	76.5	75.3	73.9
	Far	*93.4*	96.4	95.8	95.2

The column with italicized data represents the Rural values against which values from other 3 columns is compared, as all the other 3 columns belong to urban class

Trend Analysis

To statistically assess the upward or downward trend in the various extreme heat indices over the years, Mann Kendall (MK) test and Sen's slope estimator are computed for all the three time frames. These are non-parametric methods used to detect the trends in not normally distributed data and data with missing values and can also handle outliers in the data [65]. For MK test, if p value is less than the significance level $\alpha = 0.01$, the null hypothesis (H_o = there is no trend), is not accepted. Rejecting null hypothesis indicates that there is a trend in the time series at significance level of 1%. All the heat stress indices have shown the presence of trend at 99% confidence. The further analysis using Thiel-Sen's slope estimator shows that all the heat stress indices show increasing trend.

The MK test analysis for TNp95 and the hottest night indicate slightly steeper values in north, north-east and eastern parts of domain. The coldest daytime temperature shows an overall increasing trend, with slightly higher rates of increase (0.05 °C/year) for urban areas in center of domain, in comparison to rural areas (0.04 °C). Slightly higher slope values for the coldest night time temperature is observed on eastern parts of the domain (0.067 °C/year) as compared to other parts. For the hottest day temperatures, the rate of increase varies between 0.049 °C/year to 0.053 °C/year, with lower values dominating the south to south-eastern parts of study domain. The CHT index shows a peculiar trend, with greater slope for rural parts (0.42/year) than urban areas (0.3/year).

The NHWD, FHW, and IHW all show a significantly ($p < 0.01$) positive trend according to the MK test. The Theil-Sen's slope for MK shows that all the three indices have greater values for urban areas in contrast to rural areas indicating sharper increase in urban than rural areas (Fig. 7). For instance, in the city areas, NHWD is increasing at a rate of approximately 0.35–0.4/year, while for rural surroundings, the increase is at rate of 0.2–0.25/year. Similarly, for urban areas, the number of heat waves is increasing at rate of 0.02/year, while for rural areas, it is almost no increase to 0.005/year. IHW has much steeper slopes (0.11 °C/year to 0.13 °C/year) of increase in southern and south-eastern urban areas of the domain. While, in the rural parts, IHW is increasing at rates of 0.05–

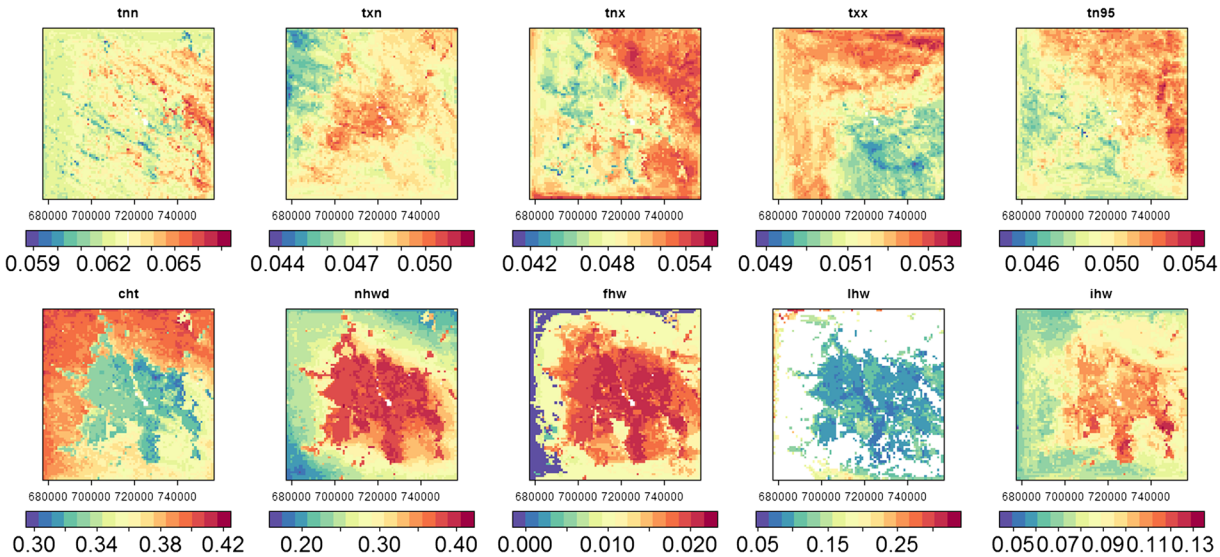

Fig. 7 Sen's slope estimator at $\alpha = 0.01$, for the coldest night (TNn), coldest day (TXn), hottest night (TNx), hottest day (TXx), warmest 5% days (TN95), combined hot days and tropical nights (CHT), number (NHWD), frequency (FHW), duration (DHW), and intensity of heat waves (IHW)

0.08 °C/year. The trend for DHW index is not uniformly significant across the domain. The trend is significantly positive only in the city areas with a slope of 0.05–0.15.

Conclusion

In the current study, we examined the urban climate of Delhi, in reference (1986–2005), near-future (2026–2045), and far-future (2081–2100) time frames with respected to the climate change, with a focus on extreme heat events. Ten extreme heat indices were used to analyze the results: the coldest night (TNn), coldest day (TXn), hottest night (TNx), hottest day (TXx), 95th percentile of daily minimum temperature (TNp95), combined hot days and tropical nights (CHT), number (NHWD), frequency (FHW), duration (DHW), and intensity (IHW) of heat waves. Based on the results, it is observed that the urban areas within the study domain on average experience 2.9 more heat wave days than their rural surroundings, and the situation is expected to worsen in future when this difference is expected to increase to 13.8 in far future under RCP8.5 climate change scenario. This is a crucial observation, as in India, a heat wave is declared using rural temperature forecasts only and only then the 'heat health action plans' are implemented. Thus, urban populations are undergoing several heat wave days with no action taken. The urban areas are also expected to face heat waves more frequently than rural areas. In reference time frame, rural areas face three heat waves on an average in 10 summer seasons, while urban areas experience one heat wave each summer season. This number is expected to rise to 4.3 for rural and 5.1 for urban areas, for each summer season. Similar trend is observed in the duration of heat waves. For instance, the duration of heat wave in rural areas is expected to increase from 3.5 (reference period) to 9.7 days (far future). While for rural areas, the duration is expected to rise from 1.6 to 7.5 days.

Though the impact of UHI is seen on the number, intensity, frequency, and duration of heat waves, however, the UHI intensity in the domain has not changed drastically over the years. The results however are useful in identifying and isolating the role of UHI in augmenting the city's vulnerability to climate change. For future research, varying land use scenario could be employed to study the impact of urbanising landscape on the UHI effect and subsequent influence on extreme climatic events under different climate change scenarios.

The results of this study can be helpful for urban managers to understand the extreme heat threats that their city will face and prepare the adaptation plans accordingly. Such work for instance could be a direct input for preparing heat action plans like that of Ahmedabad. Also, the

outcomes from this study could serve as inputs for assessing the climatic vulnerabilities of the city. Urban planners in particular can draw benefits from such studies, as these results inform them of the areas or pockets in the city under severe threat from UHI effects. The planners and landscape designers when informed about the critical areas can hence plan accordingly to minimize and mitigate the UHI and severe heat impacts.

Acknowledgments The work described in this paper has received funding from the European Community's 7th Framework Programme under Grant Agreements Nos. 308497 (RAMSES) and 308299 (NACLIM), and from the BELSPO through its Brain.be project (CORDEX.be). The authors also acknowledge the use of data from ECMWF, NCDC and NASA. The authors thankfully acknowledge the WUDAPT for using their LCZ classification methodology.

References

1. Hansen J, Sato M, Ruedy R. Perception of climate change. *Proc Natl Acad Sci*. 2012;109(37):E2415–23.
2. Ando A, Camm J, Polasky S, Solow A. Species distributions, land values, and efficient conservation. *Science*. 1998;279(5359):2126–8.
3. Hajat S, Armstrong B, Baccini M, Biggeri A, Bisanti L, Russo A, et al. Impact of high temperatures on mortality: is there an added heat wave effect? *Epidemiology*. 2006;17(6):632–8.
4. Kilbourne EM. 1997. *Heat waves and hot environments*. The public health consequences of disasters 245–269.
5. Sartor F, Snacken R, Demuth C, Walckiers D. Temperature, ambient ozone levels, and mortality during summer, 1994, in Belgium. *Environ Res*. 1995;70(2):105–13.
6. Semenza JC, Rubin CH, Falter KH, Selanikio JD, Flanders WD, Howe HL, et al. Heat-related deaths during the July 1995 heat wave in Chicago. *N Engl J Med*. 1996;335(2):84–90.
7. Knowlton K, Rotkin-Ellman M, King G, Margolis HG, Smith D, Solomon G, et al. The 2006 California heat wave: impacts on hospitalizations and emergency department visits. *Environ Health Perspect*. 2009;117(1):61–7.
8. Zander KK, Botzen WJ, Oppermann E, Kjellstrom T, Garnett ST. Heat stress causes substantial labour productivity loss in Australia. *Nat Clim Chang*. 2015;5(7):647–51.
9. IPCC. *Climate change 2013: the physical science basis. Contribution of working group I to the fifth assessment report of the intergovernmental panel on climate change*. Cambridge, United Kingdom and New York, NY, USA: Cambridge University Press; 2013.
10. Robine JM, Cheung SLK, Le Roy S, Van Oyen H, Griffiths C, Michel JP, et al. Death toll exceeded 70,000 in Europe during the summer of 2003. *C R Biol*. 2008;331(2):171–8.
11. Green HK, Andrews NJ, Bickler G, Pebody RG. Rapid estimation of excess mortality: nowcasting during the heatwave alert in England and Wales in June 2011. *J Epidemiol Community Health*. 2012;66(10):866–8.
12. Matsueda M. Predictability of Euro-Russian blocking in summer of 2010. *Geophys Res Lett*. 2011;38(6).
13. Department of Health & Human Services. *Heatwave Plan England*. 2012;2012.
14. Whitman S, Good G, Donoghue ER, Benbow N, Shou W, Mou S. Mortality in Chicago attributed to the July 1995 heat wave. *Am J Public Health*. 1997;87(9):1515–8.
15. Guirguis K, Gershunov A, Tardy A, Basu R. The impact of recent heat waves on human health in California. *J Appl Meteorol Climatol*. 2014;53(1):3–19.
16. Kysely J, Kim J. Mortality during heat waves in South Korea, 1991 to 2005: how exceptional was the 1994 heat wave? *Clim Res*. 2009;38(2):105–16.
17. Nishi M, Pelling M, Yamamuro M, Solecki W, Kraines S. Risk management regime and its scope for transition in Tokyo. J Extreme Events. 2016;3(03):1650011.
18. Azhar GS, Mavalankar D, Nori-Sarma A, Rajiva A, Dutta P, Jaiswal A, et al. Heat-related mortality in India: excess all-cause mortality associated with the 2010 Ahmedabad heat wave. *PLoS One*. 2014;9(3):e91831.
19. Masood I, Majid Z, Sohail S, Zia A, Raza S. The deadly heat wave of Pakistan, June 2015. *Int J Occup Environ Med*. 2015;6(4 October):672–247.
20. Hanna EG, Tait PW. Limitations to thermoregulation and acclimatization challenge human adaptation to global warming. *Int J Environ Res Public Health*. 2015;12(7):8034–74. https://doi.org/10.3390/ijerph120708034.
21. Anderson GB, Bell ML. Heat waves in the United States: mortality risk during heat waves and effect modification by heat wave characteristics in 43 US communities. *Environ Health Perspect*. 2011;119(2):210.
22. Kent ST, McClure LA, Zaitchik BF, Smith TT, Gohlke JM. Heat waves and health outcomes in Alabama (USA): the importance of heat wave definition. *Environ Health Persp (Online)*. 2014;122(2):151–8.
23. Alexander LV, Arblaster JM. Assessing trends in observed and modelled climate extremes over Australia in relation to future projections. *Int J Climatol*. 2009;29(3):417–35.
24. Frich P, Alexander L, Della-Marta P, Gleason B, Haylock M, Tank AK, et al. Observed coherent changes in climatic extremes during the second half of the twentieth century. *Clim Res*. 2002;19(3):193–212.
25. Alexander L, Zhang X, Peterson T, Caesar J, Gleason B, Klein Tank A, Haylock M, Collins D, Trewin B, Rahimzadeh F. 2006. Global observed changes in daily climate extremes of temperature and precipitation. *J Geophys Res: Atmosp* 111(D5).
26. Garssen J, Harmsen C, De Beer J. 2005. *The effect of the summer 2003 heat wave on mortality in the Netherlands*. Text.
27. CMA. 2012. *Heat wave. Chinese Meteorological Association*.
28. Chestnut LG, Breffle WS, Smith JB, Kalkstein LS. Analysis of differences in hot-weather-related mortality across 44 US metropolitan areas. *Environ Sci Pol*. 1998;1(1):59–70.
29. Keatinge WR, Donaldson GC, Cordioli E, Martinelli M, Kunst AE, Mackenbach JP, et al. Heat related mortality in warm and cold regions of Europe: observational study. *BMJ: Br Med J*. 2000;321(7262):670–3.

30. Dousset B, Gourmelon F, Laaidi K, Zeghnoun A, Giraudet E, Bretin P, et al. Satellite monitoring of summer heat waves in the Paris metropolitan area. *Int J Climatol*. 2011;31(2): 313–23. https://doi.org/10.1002/joc.2222.
31. Jusuf SK, Wong NH, Hagen E, Anggoro R, Hong Y. The influence of land use on the urban heat island in Singapore. *Habitat Int*. 2007;31(2):232–42.
32. Stone B, Hess JJ, Frumkin H. Urban form and extreme heat events: are sprawling cities more vulnerable to climate change than compact cities. *Environ Health Perspect*. 2010;118(10):1425–8.
33. Zhao L, Lee X, Smith RB, Oleson K. Strong contributions of local background climate to urban heat islands. *Nature*. 2014;511(7508):216–9.
34. Cheema AR. Pakistan: high-rise buildings worsened heatwave. *Nature*. 2015;524(7563):35.
35. Saeed F, Suleri AQ. *Future Heatwaves in Pakistan under IPCC's AR5 climate change scenario*. Islamabad, Pakistan: Policy Brief. Sustainable Development Policy Institute; 2015.
36. Attri S, Tyagi A. Climate profile of India. Contribution to the Indian network of climate change assessment (NATIONAL COMMUNICATION-II). *Ministry Environ Forests*. 2010;1501:1–129.
37. Knowlton K, Kulkarni PS, Azhar SG, Mavalankar D, Jaiswal A, Connolly M, et al. Development and implementation of South Asia's first heat-health action plan in Ahmedabad (Gujarat, India). *Int J Environ Res Public Health*. 2014;11(4):3473–92. https://doi.org/10.3390/ijerph110403473.
38. Guerreiro SB, Dawson RJ, Kilsby C, Lewis E, Ford A. Future heat-waves, droughts and floods in 571 European cities. Environ Res Lett. 2018;13(3):034009.
39. Adachi SA, Kimura F, Kusaka H, Inoue T, Ueda H. Comparison of the impact of global climate changes and urbanization on summertime future climate in the Tokyo metropolitan area. J Appl Meteorol Climatol. 2012;51(8): 1441–54.
40. Argüesoa, D., Evansa, J.P., Fitaa, L. and Bormannab, K.J., 2013. Simulated impact of urban expansion on future temperature heatwaves in Sydney. In 20th International Congress on Modelling and Simulation.
41. Demuzere, M., De Ridder, K. and Van Lipzig, N.P.M. 2008. Modeling the energy balance in Marseille: sensitivity to roughness length parameterizations and thermal admittance. *Journal of Geophysical Research: Atmospheres,* 113(D16).
42. De Ridder K, Lauwaet D, Maiheu B. UrbClim–a fast urban boundary layer climate model. *Urban Climate*. 2015;12:21–48.
43. García-Díez M, Lauwaet D, Hooyberghs H, Ballester J, De Ridder K, Rodó X. Advantages of using a fast urban boundary layer model as compared to a full mesoscale model to simulate the urban heat island of Barcelona. *Geosci Model Dev*. 2016;9(12):4439–50.
44. Lauwaet D, De Ridder K, Saeed S, Brisson E, Chatterjee F, van Lipzig N, et al. Assessing the current and future urban heat island of Brussels. *Urban Climate*. 2016;15:1–15.
45. Lauwaet D, Hooyberghs H, Maiheu B, Lefebvre W, Driesen G, Van Looy S, et al. Detailed urban heat island projections for cities worldwide: dynamical downscaling CMIP5 global climate models. *Climate*. 2015;3(2):391–415.
46. Danielson JJ, Gesch DB. 2011. *Global multi-resolution terrain elevation data 2010 (GMTED2010)*. US Geological Survey.
47. Bechtel B, Alexander P, Böhner J, Ching J, Conrad O, Feddema J, et al. Mapping local climate zones for a worldwide database of the form and function of cities. *ISPRS Int J Geo-Inform*. 2015;4(1):199–219.
48. Mills, G., Ching, J., See, L., Bechtel, B. and Foley, M. 2015. An introduction to the WUDAPT project. *Proceedings of the 9th International Conference on Urban Climate,* Toulouse, France (July): 20-24.
49. Gutman G, Ignatov A. The derivation of the green vegetation fraction from NOAA/AVHRR data for use in numerical weather prediction models. *Int J Remote Sens*. 1998;19(8): 1533–43.
50. Gerland P, Raftery AE, Ševčíková H, Li N, Gu D, Spoorenberg T, et al. World population stabilization unlikely this century. *Science*. 2014;346(6206):234–7.
51. Van Vuuren DP, Edmonds J, Kainuma M, Riahi K, Thomson A, Hibbard K, et al. The representative concentration pathways: an overview. *Clim Chang*. 2011;109:5–31.
52. Agarwal A, Babel MS, Maskey S, Shrestha S, Kawasaki A, Tripathi NK. Analysis of temperature projections in the Koshi River Basin, Nepal. *Int J Climatol*. 2016;36(1):266–79.
53. Donat M, Alexander L, Yang H, Durre I, Vose R, Dunn R, et al. Updated analyses of temperature and precipitation extreme indices since the beginning of the twentieth century: the HadEX2 dataset. *J Geophys Res-Atmos*. 2013;118(5): 2098–118.
54. Fischer E, Schär C. Consistent geographical patterns of changes in high-impact European heatwaves. *Nat Geosci*. 2010;3(6):398–403.
55. Klein Tank A, Peterson T, Quadir D, Dorji S, Zou X, Tang H, Santhosh K, Joshi U, Jaswal A, Kolli R. 2006. Changes in daily temperature and precipitation extremes in central and south Asia. *J Geophysic Res: Atmos* 111(D16).
56. Sheikh M, Manzoor N, Ashraf J, Adnan M, Collins D, Hameed S, et al. Trends in extreme daily rainfall and temperature indices over South Asia. *Int J Climatol*. 2015;35(7): 1625–37.
57. Vincent L, Aguilar E, Saindou M, Hassane A, Jumaux G, Roy D, Booneeady P, Virasami R, Randriamarolaza L, Faniriantsoa F. 2011. Observed trends in indices of daily and extreme temperature and precipitation for the countries of the western Indian Ocean, 1961–2008. *J Geophysic Res: Atmos* 116(D10).
58. McCarthy MP, Harpham C, Goodess CM, Jones PD. Simulating climate change in UK cities using a regional climate model, HadRM3. *Int J Climatol*. 2012;32(12):1875–88.
59. Oleson K. Contrasts between urban and rural climate in CCSM4 CMIP5 climate change scenarios. *J Clim*. 2012;25(5):1390–412.
60. Lemonsu A, Viguie V, Daniel M, Masson V. Vulnerability to heat waves: impact of urban expansion scenarios on urban heat island and heat stress in Paris (France). *Urban Climate*. 2015;14:586–605.
61. Hamdi R, Giot O, De Troch R, Deckmyn A, Termonia P. Future climate of Brussels and Paris for the 2050s under the A1B scenario. Urban Clim. 2015;12:160–82.

62. Son J-Y, Lee J-T, Gb A, Bell ML. The impact of heat waves on mortality in seven major cities in Korea. *Environ Health Perspect*. 2012;120(4):566–71.
63. Anderson BG, Bell ML. Weather-related mortality: how heat, cold, and heat waves affect mortality in the United States. *Epidemiology (Cambridge Mass)*. 2009;20(2):205.
64. Díaz J, Jordan A, Garcia R, López C, Alberdi J, Hernández E, et al. Heat waves in Madrid 1986–1997: effects on the health of the elderly. *Int Arch Occup Environ Health*. 2002;75(3):163–70.
65. Jhajharia D, Shrivastava S, Sarkar D, Sarkar S. Temporal characteristics of pan evaporation trends under the humid conditions of northeast India. *Agric For Meteorol*. 2009;149(5):763–70.